Optical and Quantum Electronics (2018) 50:411
https://doi.org/10.1007/s11082-018-1651-5

Supercontinuum generation with femtosecond optical pulse compression in silicon photonic crystal fibers at 2500 nm

Ashkan Ghanbari[1] · Alireza Kashaninia[1] · Ali Sadr[2] · Hamed Saghaei[3]

Received: 24 July 2018 / Accepted: 29 September 2018 / Published online: 30 October 2018

Abstract
In this paper, femtosecond optical pulses compression and supercontinuum generation in a triangular silicon photonic crystal fiber at 2500 nm are investigated. A region of large minimum anomalous group velocity dispersion, negligible higher order dispersions and unique nonlinearity of silicon are used to demonstrate compression of 100 fs initial input optical pulses to 2.5 fs and ultra-broadband supercontinuum generation with very low input pulse energy over short distances of the fiber.

Keywords Soliton · Compression · Dispersion · Photonic · Crystal

1 Introduction

According to the appearance of the applications in several fields of the sciences, researches and technologies, ultrashort optical pulses generation has been considered an interesting topic among scientists. The accessibility of these ultrashort laser pulses has opened numerous regions of applications in many applicable optical fields, such as spectroscopy, nonlinear optics, Optical Coherent Tomography (OCT), precious optical measurement of optical frequencies, material process and etc. (Ferreira 2011). Ultrashort femtosecond laser pulses have been generated either from different optical laser sources such as Ti:sapphire

✉ Alireza Kashaninia
ali.kashaniniya@iauctb.ac.ir

Ashkan Ghanbari
ashkan.ghanbari@iauctb.ac.ir

Ali Sadr
sadr@iust.ac.ir

Hamed Saghaei
h.saghaei@iaushk.ac.ir

1 Department of Electrical Engineering, Faculty of Engineering, Central Tehran Branch, Islamic Azad University, Tehran, Iran

2 Faculty of Electrical and Electronics Engineering, Iran University of Science and Technology (IUST), Tehran, Iran

3 Department of Electrical Engineering, Shahrekord Branch, Islamic Azad University, Shahrekord, Iran

oscillators (800 nm), Er:fiber laser (1550 nm), Nd:YAG lasers (1064 nm) (Ghanbari et al. 2017) and Cr^{+2}:ZnSe laser (2500 nm) (Cizmeciyan et al. 2013) or by spectral extending of the optic pulse and post compression using dispersion compensating fundaments (Mohebbi 2008).

Ultrashort optical pulses generation directly from laser sources require more complex activity such as, cavity and dispersion compensating mirrors designs and also use of enhanced optical pulses with energy in micro joule ranges (Ferreira 2011; Mohebbi 2008). One of the most widely used techniques for the generation of ultrashort optical pulses uses higher order solitons which are organized in a fiber. This compression method named soliton-effect and has been used in many researches (Ferreira 2011).

Recently, photonic crystal fibers have been attracted the attention of many scientists and researchers for their highly precious applications in lasers, nonlinear optics, dispersion compensation, optical amplifiers, optical sensors and etc. (Ferreira 2011; Cizmeciyan et al. 2013; Mohebbi 2008; Saghaei 2015) and also several types of fabricating with variable materials have been reported so far (Saghaei 2015; Ghanbari et al. 2017; Li and Yaman 2010; Leong et al. 2006; Bowmans et al. 2003). Because of the presence of air holes in the various lattice structures of photonic crystal fibers, acquiring various optical properties such as Large Mode Area (LMA), high nonlinearity, adjustable zero dispersion and etcetera become possible in comparison with conventional optical fibers (Ghanbari et al. 2017; Li and Yaman 2010; Ghanbari 2012). Among the items mentioned above, the combination of boosted nonlinearity and engineered dispersion is the one which makes the soliton-effects optical pulses compression and ultra-broadband supercontinuum generation possible in a broad regions of wavelengths from visible to infrared in different kinds of PCFs (Saghaei 2015; Ghanbari et al. 2014, 2017; Ghanbari 2012). Photonic crystal fibers can be made from different optical materials such as silica (Leong et al. 2006), fluoride magnesium (Ghanbari et al. 2017), chalcogenide glasses (Saghaei 2015) and also silicon (Li and Yaman 2010). Today silicon is known as one of the most important and well known materials for fabrication of optoelectronic instruments (Mohebbi 2008; Li and Yaman 2010). Recently, silicon photonic crystal fibers have been fabricated by a special method named "magnesium thermic method" with the ability to maintain the Nano scales dimensions of the related silicon fibers (Li and Yaman 2010). Based on our researches, silicon has larger nonlinear refractive index than silica, chalcogenide glasses and also fluoride magnesium (Saghaei 2015; Ghanbari et al. 2017; Bowmans et al. 2003). Finally, this valuable nonlinear refractive index results in obtaining higher nonlinear coefficient and subsequently lower required input pulse energy for nonlinear applications such as optical compression or supercontinuum generation.

In this paper, we focused on designing a novel structure of photonic crystal fiber consisting of a silicon core surrounded by five rings of air holes embedded in a triangular lattice in the cladding and we also used the soliton-effect method for compression of femtosecond optical pulses and ultra-broadband supercontinuum generation.

2 Dispersion of silicon photonic crystal fibers

Dispersion is one of the most important linear parameters that affects the short and ultrashort pulses propagation which causes optical pulses broadening in the time domain (Mohebbi 2008). By changing the structural parameters of photonic crystal fibers such as wavelengths (λ), hole pitch (Λ) and normalized air hole diameter ($^{d}/_{\Lambda}$), PCF's dispersion can change. Also Shifting zero dispersion points in photonic crystal fibers are possible by dependency of group velocity dispersion (GVD) to structural parameters of PCFs (Ferreira 2011; Saghaei 2015; Ghanbari et al. 2017).

As seen in Fig. 1, we considered a triangular lattice silicon PCF with five rings of air holes in the cladding. In the center an air hole is deleted making a central high index defect acting as the PCF core. In order to calculate propagation constant (β) for the proposed silicon PCF, among all the accurate available techniques, we selected one of the well-known numerical methods named Finite Difference Time Domain (FDTD) combined with the perfectly matched layer (PML) as absorbing boundaries (Saghaei 2015; Ghanbari et al. 2017). The second and higher order dispersions of the fiber can be calculated by taking the first, second and higher orders derivative of the propagation constant with respect to angular frequency as following equation respectively (Ferreira 2011; Mohebbi 2008). Where dependency of the silicon material has been also applied into the calculations (Ghanbari 2012; Lin and Agrawal 2007),

$$\beta_n = {}^{\partial \beta_{n-1}}\big/_{\partial \omega} \quad \mathrm{n} = 2, 3, 4, \ldots \tag{1}$$

In Fig. 2, we have shown the GVD as a function of wavelength in the short wavelength infrared (SWIR) and mid infrared (MIR) regions of the spectrum for the largest possible value of normalized air hole size (${}^{d}/_{\Lambda} = 0.8$) and different values of pitches (Λ). As seen in Fig. 2, there is a nearly flat and minimum region of negative second order dispersion (GVD) which by changing the hole pitch (Λ) is shifted to higher wavelengths. So by choosing the proper values of $\Lambda = 0.7$ µm and ${}^{d}/_{\Lambda} = 0.8$, this negative and nearly flat region of GVD can be centered at 2500 nm wavelength. The importance of nearly flat region in supercontinuum generation and soliton-effect pulse compression contributes to achieving negligible higher order dispersions.

When we consider the propagation of ultrashort optical pulses with femtosecond durations, the higher order dispersions (HODs) (such as third, fourth, fifth and etc.) will be of great importance and must be included in the wave equation. In Fig. 3 we have shown the third (TOD), fourth (FOD) and fifth order dispersions of the fiber as a function of wavelength for ${}^{d}/_{\Lambda} = 0.8$ and $\Lambda = 0.7$ µm. This figure clearly shows that in the similar region of wavelengths where there is a large minimum and nearly flat negative second order dispersion, the values of higher order dispersions in the novel designed silicon PCF will be

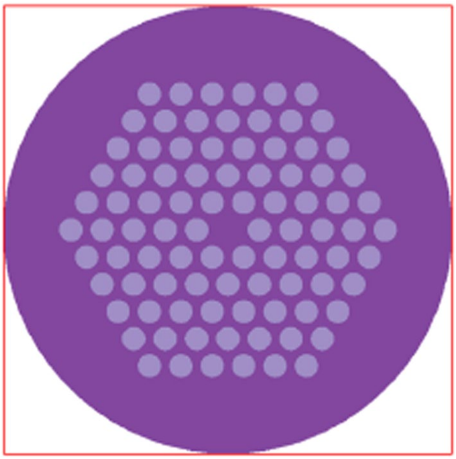

Fig. 1 Silicon PCF schematic

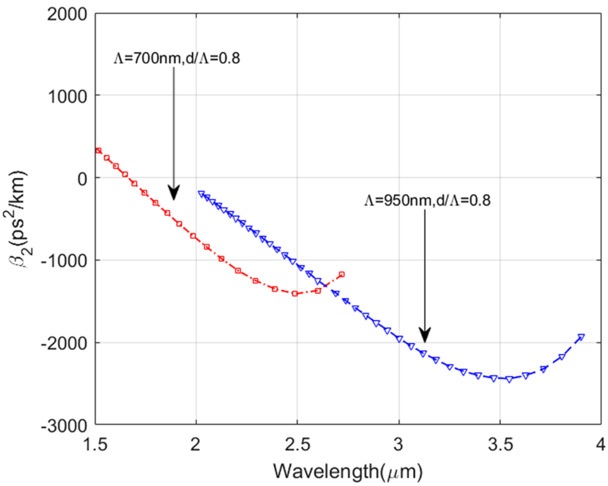

Fig. 2 GVD of silicon PCF as a function of wavelength for ${}^{d}/_{\Lambda} = 0.8$ and two pitches

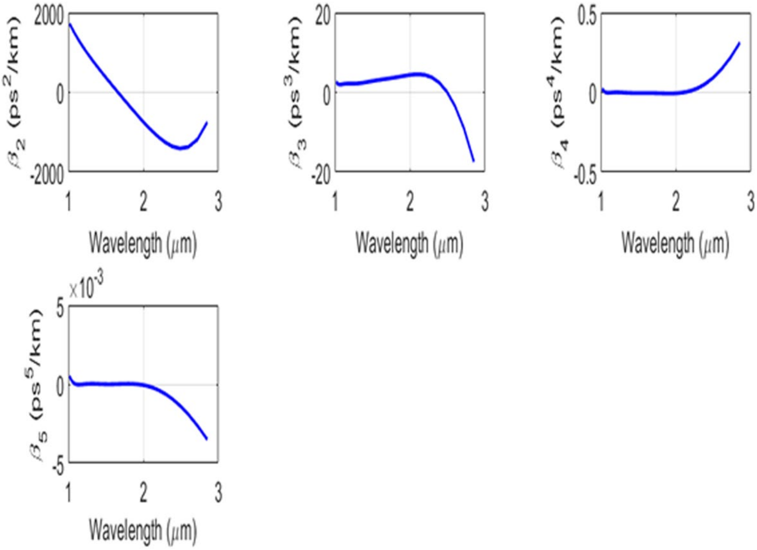

Fig. 3 Up to fifth order dispersions of silicon PCF as a function of wavelength for $\Lambda = 0.7$ μm and ${}^{d}/_{\Lambda} = 0.8$

negligible compared to the value of GVD, which are ideally needed for supercontinuum generation and soliton-effect compression. But it is noteworthy that although these higher order dispersions values are small at 2500 nm wavelength, they should be considered in the wave equation. Another important linear parameter which can affect the propagated pulse inside the fiber is fiber loss ($L_t = L_c + L_m$) (Saghaei 2015; Ghanbari et al. 2017). Total loss of the fiber includes material loss and confinement loss respectively. Based on our research and simulation results, the silicon PCF confinement Loss could be negligible compared to the material loss of silicon according to presence of air holes in the cladding. So, for the rest of the paper we considered the silicon material loss with the value of 8 ${}^{\mathrm{db}}/_{\mathrm{m}}$ (Luther et al. 2013) at the central wavelength of 2500 nm in the accounts.

3 Soliton-effect compression in silicon photonic crystal fibers

In this kind of optical pulse compression mechanism, the waveguide, itself, acts as a compressor. In fact, soliton-effect optical pulse compression occurs through the propagation of higher order solitons in the anomalous GVD regions of the fiber and interact with self-phase modulation (SPM). In this case by choosing the appropriate length of the fiber where the pulse goes under periodic compressing, we can select the ultrashort output pulse.

Figure 4, shows the effective areas of silicon designed PCF for the structure parameters of $\Lambda = 0.7$ µm, $^{d}/_{\Lambda} = 0.8$ and $\Lambda = 0.95$ µm, $^{d}/_{\Lambda} = 0.8$ respectively. The Combination of unique nonlinear refractive index of silicon (n2) with a small effective area, finally results in higher nonlinear index ($\gamma \propto {}^{1}/_{A_{eff}} \propto n_2$). Smaller effective area can be achieved by designing photonic crystal fibers with smaller pitches (Λ). Also smaller effective area leads to a shorter nonlinear length (L_{NL}). Ultimately, all of the items above contribute to a conspicuous reduction in required energy for PCF's nonlinear applications. As seen in Fig. 4, the effective area for the proposed silicon PCF with the structure parameters of $\Lambda = 0.7$ µm and $^{d}/_{\Lambda} = 0.8$ is calculated to be 0.52 µm^2 at 2500 nm wavelength which is much smaller than the effective area of proposed PCF with the structure parameters of $\Lambda = 0.95$ µm and $^{d}/_{\Lambda} = 0.8$ at 3500 nm wavelength which is calculated to be 1 µm^2.

The Generalized Nonlinear Schrödinger Equation which describes the propagation of optical pulses through fibers can be written in the following normalized form (Saghaei 2015; Ghanbari et al. 2014, 2017; Ghanbari 2012),

$$\frac{\partial U}{\partial \xi} = \overbrace{-\frac{isgn(\beta_2)}{2}\frac{\partial^2 U}{\partial \tau^2} + \frac{\beta_3}{6|\beta_2|T_0}\frac{\partial^3 U}{\partial \tau^3} + i\frac{\beta_4}{24|\beta_2|T_0^2}\frac{\partial^4 U}{\partial \tau^4} - \frac{\beta_5}{120|\beta_2|T_0^3}\frac{\partial^5 U}{\partial \tau^5}}^{Linear\text{ - Effects}} + \cdots + {}^{L_D\alpha_L}/_{2}U$$
$$\underbrace{+ iN^2(\underbrace{|U|^2}_{SPM} U + \underbrace{\frac{i}{\omega_0 T_0}}_{Self-steepening}\frac{\partial(|U|^2U)}{\partial \tau} - \underbrace{{}^{U}/_{T_0 f_R}\int_0^\infty th_R(t)dt\frac{\partial |U|^2}{\partial \tau})}_{RAMAN}}_{Nonlinear-effects} - \underbrace{{}^{N^2\alpha_{TPA}}/_{2\gamma A_{eff}}U|U|^2}_{TPA} \tag{2}$$

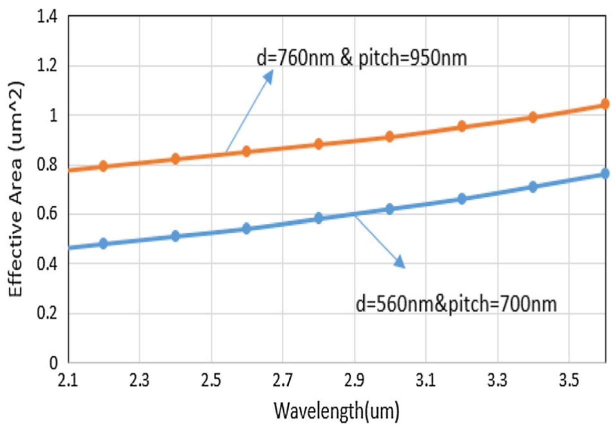

Fig. 4 Effective area of the fundamental mode for a silicon PCF

where $\tau = {}^{T}/{}_{T_0}$ is the normalized time, T0 states the initial pulse width of optical pulses ($T_{FWHM} = 1.76T_0$), T_{FWHM} states full width at half maximum of the optical pulse, and $U(z,\tau) = {}^{A(z,\tau)}/{}_{\sqrt{P_0}}$ is the normalized pulse amplitude, P0 is the peak power of input pulse, $\alpha(m^{-1})$ is linear loss coefficient,$\beta_2, \beta_3, \beta_4, \beta_5$ are GVD, TOD, FOD and Fifth order dispersions respectively. ω_0 is the central angular frequency, ${}^{1}/{}_{\omega_0 T_0}$ is responsible for self-steepening, f_R is Raman constant and is calculated 0.04 for silicon material (Ghanbari 2012; Luther et al. 2013; Lin and Agrawal 2007). $h_R(t)$ is Raman Function and can be calculated by definition of $\tau_1 = 10$ fs and $\tau_2 = 3$ ps for silicon material in the following formula (Mohebbi 2008),

$$h_R(t) = \frac{\tau_1^2 + \tau_2^2}{\tau_1 \tau_2^2} e^{\frac{-t}{\tau_2}} \sin({}^{t}/{}_{\tau_1}) \tag{3}$$

N^2 is the order of soliton and defined as,

$$N^2 = \frac{\gamma P_0 T_0^2}{|\beta_2|} \tag{4}$$

where, γ states the nonlinear coefficient defined by Eq. (4),

$$\gamma = \frac{n_2 \omega_0}{cA_{eff}} \tag{5}$$

where $n_2\left({}^{\mathrm{m}^2}/{}_{\mathrm{W}}\right)$ is the nonlinear refractive index with the value of $3.3 \times 10^{-18}\ {}^{\mathrm{m}^2}/{}_{\mathrm{W}}$ for silicon at operational wavelength of 2500 nm (Mohebbi 2008; Yue et al. 2012), A_{eff} is the

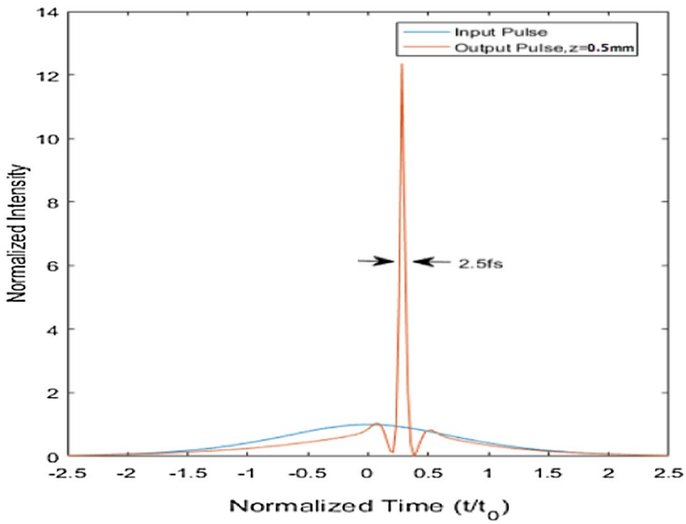

Fig. 5 Output compressed pulse at the wavelength of 2500 nm and propagation distance of 0.5 mm. Input pulse is also shown

effective area of the PCF, c shows the speed of light and finally $\xi = {}^{z}/_{L_D}$ is the normalized distance of the fiber, Where L_D is the dispersion length defined by the following equation,

$$L_D = \frac{T_0^2}{|\beta_2|} \tag{6}$$

The longer Dispersion length is, the shorter compressed pulse goes. It means that by choosing proper PCF fundamental parameters, we can make the second order dispersion (β_2) minimum at the wavelength of 2500 nm which leads to longer dispersion length (corresponds to a longer soliton period) compared to shorter wavelengths. In this manner, the condition of $L_D >> L_{NL}$ is satisfied which finally results in shorter compressed pulse. Also it is noteworthy that because of the lower magnitude of Raman response in silicon material compared to magnitude of another nonlinear effects such as SPM and self-steepening, the Raman Effect can be negligible, however, we have included it in the propagation equation. α_{TPA} is responsible for two photon absorption which limits the nonlinear effects of the silicon fibers. This important item appears for the wavelengths below 2300 nm in silicon material (Ghanbari 2012; Mohebi and Khormai 2011). So, by choosing the operational wavelength above the mentioned wavelength, this effect will be eliminated.

The widely used Symmetrized Split-Step Fourier Method (S-SSFM) is applied to simulate the Generalized Nonlinear Schrödinger Equation (GNLSE). We considered $\Lambda = 0.7$ µm and ${}^{d}/_{\Lambda} = 0.8$ for a silicon photonic crystal fiber structure and used a 100 fs

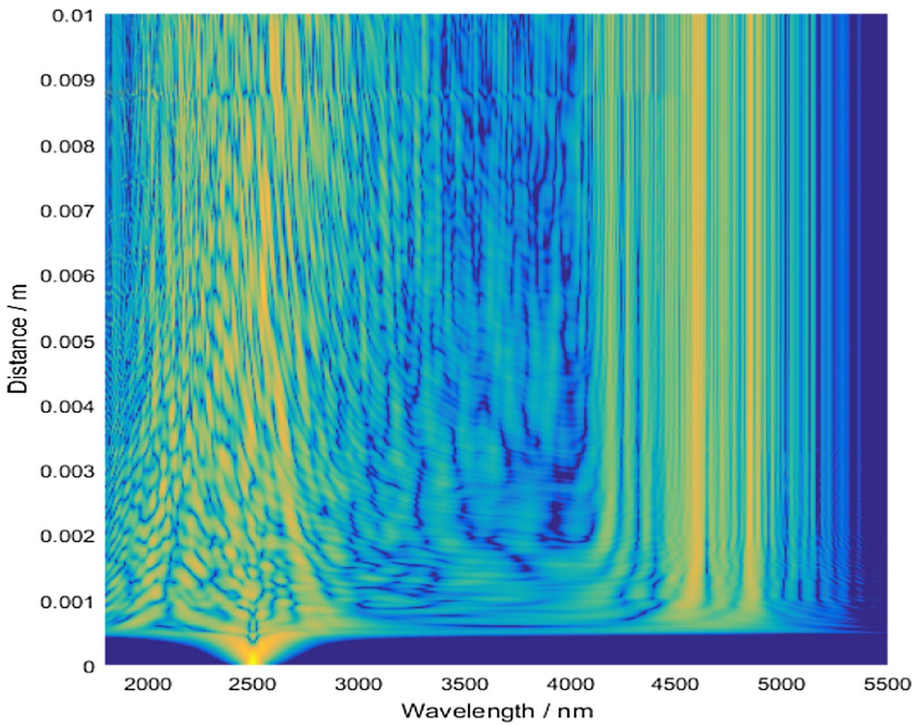

Fig. 6 Simulated 2D plot of the spectra evolution at discrete locations along the silicon PCF with the input power of 846 W

input pulse at a pump wavelength of 2500 nm. The application of GVD, TOD, FOD and fifth-order order dispersions, Self-Phase Modulation (SPM), linear loss, Self-Steepening (SS) and Raman Effect in Generalized Nonlinear Schrödinger Equation (GNLSE) simulation, yields the shortest compressed pulse of 2.5 fs which is shown in Fig. 5. This is due to the motivation of a higher order soliton of order N = 9.5 for a peak power of P_0 = 846 W, and large nonlinear coefficient of γ=16.0 (W^{-1} m^{-1}) in the propagation distance of z = 0.5 mm. The spectra evolution of propagated optical pulse over 0.01 m of the proposed silicon PCF is shown in Fig. 6. This figure clearly shows the ultra-broadband supercontinuum generation with the total bandwidth of 3600 nm in a way which covers near infrared to mid infrared regions of the spectrum. This fact is equivalent to extending the wavelength range from 1800 to 5400 nm. Wider supercontinuum spectra with the total bandwidth of 4100 nm can also be generated in the same distances of the PCF with an increase in input power to 1350 W which is shown in Fig. 7. In this case, supercontinuum spectra have been propagated with an increase of about 500 nm bandwidth compared to the previous one.

3.1 Comparison between proposed PCF characteristics with other works

In following part, widespread comparisons between our novel designed silicon PCF's structural characteristics and propagation characteristics with previous works are presented in the forms of Tables 1 and 2.

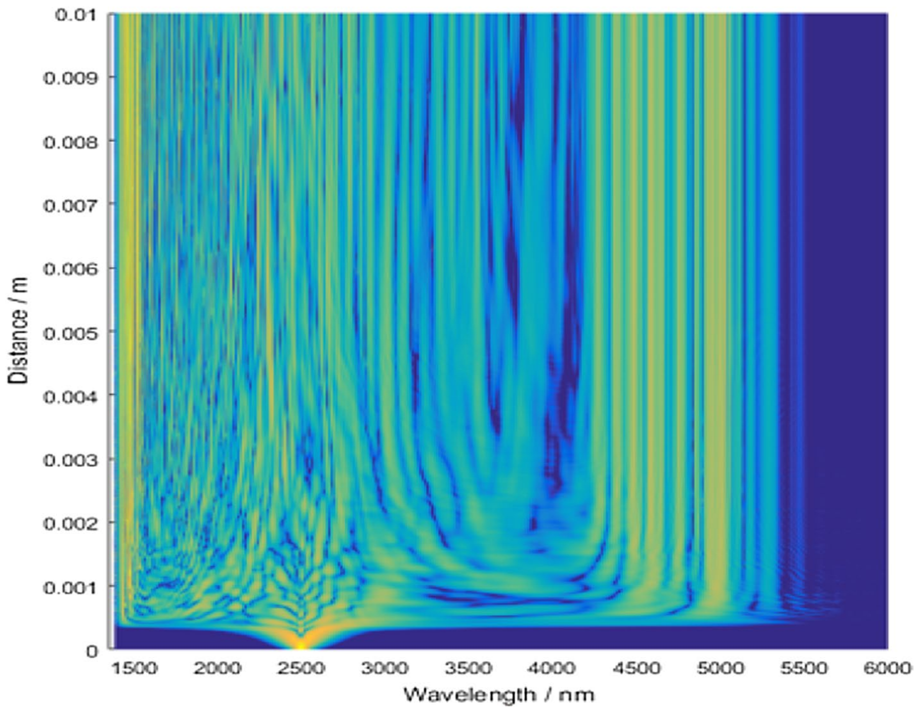

Fig. 7 Simulated 2D plot of the spectra evolution at discrete locations along the silicon PCF with input power of 1350 W

Table 1 Compasrison between proposed PCF structural parameters and other works

Info/ref	This work	(Raja et al. 2010)	(Ghanbari et al. 2015)	(Ferreira 2011)	(Cerif and Zghal 2011)	(Saghaei et al. 2012)	(Saghaei and Ghanbari 2017)
Types of fiber	Silicon	Silica	Silica	Silica	Silica	Silica	Silica
$\beta_2\left(ps^2/km\right)$	≈ −1500	− 10.5	− 147	− 12.7	− 9	− 6.33	5.53
$\beta_3\left(ps^3/km\right)$	0	0.037	0	0.08	0.07	− 0.0015	0.057
$\beta_4\left(ps^4/km\right)$	0.069	1.06e−3	Not listed	− 1.32e−4	− 1e−4	1.5e−5	1.6e−5
$\beta_5\left(ps^5/km\right)$	− .001	Not listed	Not listed	3.03e−7	2.0e−7	Not listed	− 3e−8
λ (nm)	2500	850	1550	850	850	820	532
A_{eff} (μm^2)	0.52	1.55	2.8	4.3	3	11.8	0.38
Info/ref	Ghanbari et al. (2013)	Ghanbari et al. (2017)	Ahamad (2016)	Saghaei et al. (2015)	Anitha and Manimegalai (2013)	Maggie and Chen (2011)	Ahamad (2016)
Types of fibers	Silica-PCF	MgF2	Arsenic sulfide	Chalcogenide	Silica	Silica	Arsenic selenide
$\beta_2\left(ps^2/km\right)$	− 18.15	− 8.9	− 10.7	90	− 37.4	69.7	− 31.3
$\beta_3\left(ps^3/km\right)$	0.0012	− 4.48e−3	1.4	2.33	Not listed	− .025	3
$\beta_4\left(ps^4/km\right)$	2.09e−4	1.03e−4	− 3.9e−3	− 1e−2	Not listed	Not listed	− 1e−2
$\beta_5\left(ps^5/km\right)$	− 7.734e−7	− 3.2e−7	2.1e−5	9.9e−5	Not listed	Not listed	7e−5
λ (nm)	850	640	2000	3600	1550	800	2500
A_{eff} (μm^2)	1.14	0.8	3.9	20	20	Not listed	4

Table 2 Compasrison between porposed PCF propagation characteristics and other works

Refs.	Year	Types of fiber	Full width at half maximum (TFWHM)	Output compressed pulse width	Spectrum band width	Wavelengths (nm)	Energy (J)/ soliton-order/ power (W)
Ahamad (2016)-1	2016	Arsenic sulfide-PCF	50 fs	Not listed	2200 nm	2000	5000 W
Ahamad (2016)-2	2016	Arsenic selenide-PCF	50 fs	Not listed	9000 nm	2500	20000 W
Ahamad (2016)-3	2016	PBG-PCF	50 fs	Not listed	1500 nm	1560	10000 W
Raja et al. (2010)	2010	Silica-PCF	100 fs	12 fs	Not listed	850	N = 7
Dimitre et al. (2005)	2005	PBGF	120 fs	50 fs	Not listed	1500	225 nJ
Mohebbi (2008)	2011	Nanowie-silicon	100 fs	6.5 fs	Not listed	1500	N = 6.5
Maggie and Chen (2011)	2011	Silica-PCF	1.64 ps	0.357 ps	Not listed	1554	1000 W
Ghanbari et al. (2013)	2013	Silica PCF	50 fs	4.5 fs	Not listed	850	1322 W
Ghanbari et al. (2017)	2017	MgF2	50 fs	Not listed	580 nm	640	10000 W
Saghaei and Ghanbari (2017)	2017	silica	100 fs	Not listed	830 nm	532	5000 W
Ghanbari et al. (2015)	2015	silica	300 fs	20 fs	Not listed	1550	510 pJ
Diuf et al. (2017)	2017	Chalcogenide PCF	88 fs	Not listed	1675 nm	3700	880 W
This work-1	2018	Silicon PCF	176 fs	2.5 fs	3600 nm	2500	846 W
This work-2	2018	Silicon PCF	176 fs	Not listed	4100 nm	2500	1350 W

Table 1 is allocated to our proposed PCF's structure characteristics and Table 2 is allocated to propagation characteristics of the designed fiber. Comparing the parameters clearly indicate that, the silicon designed PCF in comparison with other designs shows more ideal situation in nonlinear applications especially in supercontinuum generation and soliton-effect optical pulses compression. Our designed PCF illustrates a large minimum negative GVD and negligible higher order dispersions (HODs) values in addition to a unique nonlinear coefficient in comparison with other works. Consequently, these valuable features result in enhancing the quality of output compressed pulses, ultra-broadband supercontinuum generation and also a drastic decrease in required energy for nonlinear applications.

4 Conclusion

In this paper, for the first time, we numerically investigated the soliton-effect compression of femtosecond optical pulses and supercontinuum generation in a novel designed silicon PCF in the near mid infrared (NIR) to mid infrared (MIR) regions of the spectrum. It was shown that by fixing the fundamental parameters of the PCF, we can concentrate a large negative minimum and nearly flat region of GVD at needed wavelengths and finally calculate the negligible higher-order dispersions which are always desired for efficient ultra-broadband supercontinuum generation and femtosecond optical pulses compression. We illustrated that, by using a 100 fs input pulse with subnanojoule energy of 169 pJ (corresponds to peak power of 846 W), a compressed pulse of 2.5 fs and ultra-broadband supercontinuum with the total bandwidth of 3600 nm can be generated for a silicon PCF with considering,$\Lambda = 0.7$ µm and $^{d}/_{\Lambda} = 0.8$ at the operational wavelength of 2500 nm and the propagation distance of 0.5 mm. Also it was shown that, by increasing the strength of input power to 1350 W, ultra-broadband supercontinuum with the total band width of 4100 nm can be formed in the similar distances of the fiber.

References

Ahamad, R.: Mid infrared super-continuum generation in photonic crystal fibers. MSc Thesis, CzechTechnical University (2016)

Anitha, P., Manimegalai, A.: Ultra short pulse generation at 1550 nm using a tapered PCF. Int. J. Comput. Appl. **74**(7), 11–13 (2013)

Bowmans, G., Bigot, L., Lopez, F., Douay, M.: Fabrication and characterization of an all solid 2D photonic band gap fiber with a low loss region around 1550nm. Opt. Exp **13**(21), 8452–8459 (2003)

Cerif, R., Zghal, M.: Nonlinear phenomena ultra-wide band radiation in a photonic crystal fiber. J. Opt. **26**(17), 1–7 (2011)

Cizmeciyan, M.N., Kim, J.W., Bae, S., Hong, B.H., Routermund, F., Sennarouglu, A.: Graphene mode-locked femtosecond cr:znse at 2500 nm. JOSA **38**(3), 341–343 (2013)

Dimitre, G.O., Hensley, J., Geata, A.L., Gallagher, M.T.: Soliton pulse compression in photonic band gap fibers. Opt. Exp. **13**(16), 6153–6159 (2005)

Diuf, M., Salem, A.B., Cherif, R., Saghaei, H.: Super flat coherent supercontinuum source in AS38.8Se61.2 chalcogenide photonic crystal fiber with all normal dispersion engineering at very low input energy. Appl. Opt. **56**(2), 163–169 (2017)

Ferreira, M.F.S.: Nonlinear Effects in Optical Fibers. Wiley, Hoboken (2011)

Ghanbari, A.: Femtosecond optical pulses compression by use of photonic crystal fibers. M.Sc. Thesis, Islamic Azad University of Qazvin (2012)

Ghanbari, A., Sadr, A., Nikoo, M.: Maximization of compression factor and bandwidth of femtosecond optical pulses by use of frequency chirping in photonic crystal fibers. TJEE **43**(2), 32–41 (2013)
Ghanbari, A., Sadr, A., Tathesari, H.: Modeling photonic crystal fibers for efficient soliton effect compression pf femtosecond optical pulses at 850nm. Arab. J. Sci. Eng. **39**(5), 3917–3923 (2014)
Ghanbari, A., Kashani Nia, A., Sadr, A.: Square lattice elliptical core photonic crystal fiber soliton-effect compressor at 1550 nm. JCE **4**(1), 29–40 (2015)
Ghanbari, A., Kashani Nia, A., Sadr, A., Saghaei, H.: Supercontinuum generation for optical coherence tomography using magnesium fluoride photonic crystal fiber. Optik **140**(114), 545–554 (2017)
Leong, J.Y.Y., Asimakis, S., Polleti, F., Petropoulous, P., Feng, X., Moore, R., Frampton, K., Ebendorff-Hedepriem, H., Richardson, D.J.: Novel Fabrication Method of Highly-Nonlinear Silica Holey Fibers, pp. 21–25. CLEO, Callifornia (2006)
Li, G., Yaman, F.: *Silicon Photonic Fiber and Method of Manufacture*, No. 0092141. United States (US) Patent Application Publication (2010)
Lin, L.Y.Q., Agrawal, G.P.: Soliton fission and supercontinuum generation in silicon waveguides. Opt. Lett. **32**(4), 391–394 (2007)
Luther, B., Kuyken, B., Yu, I., Ma, P., Gai, X., Madden, S., Baets, R.: Nonlinear absorption in silicon at mid-infrared wavelengths. In: JOSA Conference Paper (2013)
Maggie, C.Y., Chen, R.T.: One stage pulse compression at 1554 nm through highly anomalous dispersive photonic crystal fiber. Opt. Exp. **19**(22), 21809–218011 (2011)
Mohebbi, M.: Silicon photonic nanowire soliton-effect compressor at 1.5μm. IEEE Photonics Technol. Lett. **20**(11), 921–924 (2008)
Mohebi, M., Khormai, H.: Effects of higher order dispersions on soliton-effect pulse compression in a silicon photonic nanowire. In: IEEE Conference (2011)
Raja, R.V., Porsezian, K., Varshney, S.K.: Modeling photonic crystal fiber for efficient soliton pulse propagation at 850 nm. Sci. Direct **39**(5), 5000–5006 (2010)
Saghaei, H., Ghanbari, A.: White light generation using photonic crystal fiber with sub-micron circular lattice. J. Electr. Eng. **68**(4), 282–289 (2017)
Saghaei, H.: Modeling and simulation of nonlinear effects in dispersion engineered photonic crystal fibers for supercontinuum generation. Ph.D. Thesis, Islamic Azad Univesrity, Science and Research Branch, Tehran (2015)
Saghaei, H., Koohi-kamali, F., Ebnali-Heidari, M., Moravvej-Farshi, M.K.: Super-Continuum Generation in Photonic Crystal Fiber Using Selective Opto-Fluidic Infiltration, pp. 106–110. ICOP, Tabriz (2012)
Saghaei, H., Heidari, M.E., Farshi, K.M.: Mid infrared super-continuum generation via As2se3 chalcogenide photonic crystal fibers. Appl. Opt. J. **54**(8), 2072–2079 (2015)
Yue, Y., Zhang, L., Huang, H.: Silicon-on-nitride waveguide with ultralow dispersion over an octave-spanning mid-infrared wavelength rang. IEEE Photonic J. **4**(1), 126–132 (2012)